

1 **Bioreactor with electrically deformable curved membranes for**  
2 **mechanical stimulation of cell cultures**

3 **Joana Costa<sup>1,2</sup>, Michele Ghilardi<sup>3,4</sup>, Virginia Mamone<sup>2,5</sup>, Vincenzo Ferrari<sup>2,5</sup>, James J.C.**  
4 **Busfield<sup>3,4</sup>, Arti Ahluwalia<sup>1,2</sup>, Federico Carpi<sup>6\*</sup>**

5 <sup>1</sup>Research Center "E. Piaggio", University of Pisa, Pisa, Italy

6 <sup>2</sup>Department of Information Engineering, University of Pisa, Pisa, Italy

7 <sup>3</sup>School of Engineering And Materials Science, Queen Mary University of London, London, UK

8 <sup>4</sup>Materials Research Institute, Queen Mary University of London, London, UK

9 <sup>5</sup>EndoCas Center for computer-assisted surgery, University of Pisa, Pisa, Italy

10 <sup>6</sup>Department of Industrial Engineering, University of Florence, Florence, Italy

11 **\*Correspondence:**  
12 Federico Carpi  
13 federico.carpi@unifi.it  
14

15

16 Frontiers in Bioengineering and Biotechnology, January 2020 |  
17 Volume 8 | Article 22

18

19 **ACCEPTED VERSION**

20

21

22 **Keywords:** actuator, bioreactor, cell, dielectric elastomer, electroactive polymer, mechanical  
23 stimulation, membrane, stretch

24 **Number of words:** 3882

25 **Number of figures:** 4

## 26 **Abstract**

27 Physiologically relevant in vitro models of stretchable biological tissues, such as muscle, lung,  
28 cardiac and gastro-intestinal tissues, should mimic the mechanical cues which cells are exposed to in  
29 their dynamic microenvironment in vivo. In particular, in order to mimic the mechanical stimulation  
30 of tissues in a physiologically relevant manner, cell stretching is often desirable on surfaces with  
31 dynamically controllable curvature. Here, we present a device that can deform cell culture  
32 membranes without the current need for external pneumatic/fluidic or electrical motors, which  
33 typically make the systems bulky and difficult to operate. We describe a modular device that uses  
34 elastomeric membranes, which can intrinsically be deformed by electrical means, producing a  
35 dynamically tuneable curvature. This approach leads to compact, self-contained, lightweight and  
36 versatile bioreactors, not requiring any additional mechanical equipment. This was obtained via a  
37 special type of dielectric elastomer actuator. The structure, operation and performance of early  
38 prototypes are described, showing preliminary evidence on their ability to induce changes on the  
39 spatial arrangement of the cytoskeleton of fibroblasts dynamically stretched for 8 hours.

40

41

## 42 **1 Introduction**

43 All biological tissues are subjected to internal mechanical forces that arise from interstitial flows and  
44 cellular motions. These forces can redistribute effector molecules that are secreted by cells, resulting  
45 in the coupling of chemical and mechanical signalling. This phenomenon, known as  
46 mechanotransduction, is a major research interest in the fields of regenerative medicine and tissue  
47 engineering (Griffith et al. 2006).

48 Static or cyclic and axial or biaxial strains applied to monolayers of cells, cultured on deformable  
49 membranes or 3D scaffolds (Elsaadany et al. 2017), have been used for decades (Meikle et al. 1979;  
50 Leung et al. 1977) to show that mechanical stretch can induce cell proliferation, increase tissue  
51 organization and enhance mechanical properties of cultured tissues. At present, most of the  
52 commercially available devices for cell stretching in vitro are actuated by pneumatic systems, such as  
53 those from Flexcell® (Flexcell International, 2019), or mechanical motors, such as those from  
54 Strex® (Strex, 2019). They require external driving units (vacuum pumps or motors), which make  
55 the systems bulky, complex to operate, acoustically noisy and generally capable of low throughput  
56 (Brown 2000).

57 Other systems are designed to mechanically stimulate cells at the microscopic scale, so as to study  
58 the response of few or even single cells, with so-called organ-on-a-chip devices (Akbari and Shea  
59 2012,a; Akbari and Shea 2012,b; Clark et al. 2000; Kim et al. 2012; Pavesi et al. 2015). They are  
60 based on microfluidic systems, which advantageously host cells in highly miniaturised chambers,  
61 although they are still limited by the need for much bulkier external fluidic components.

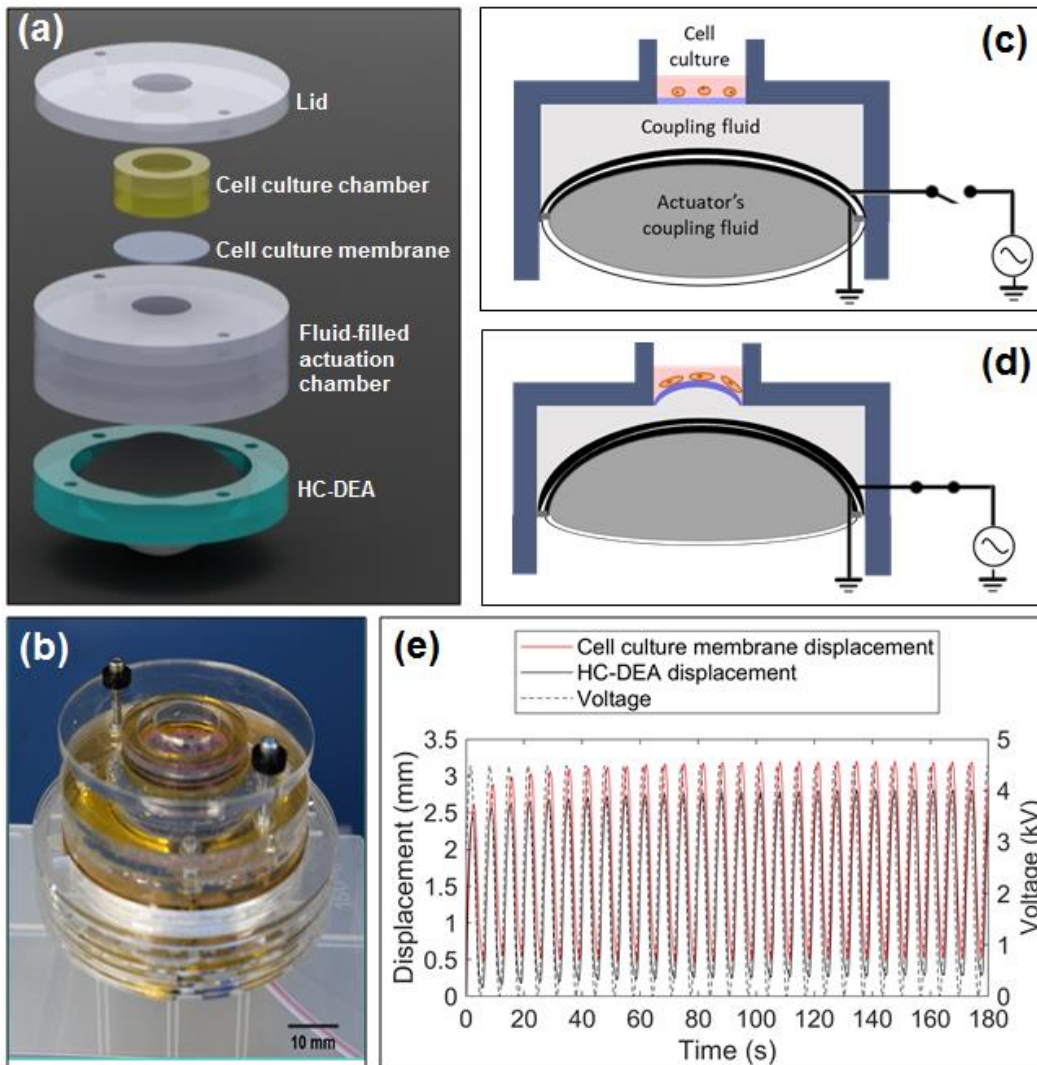
62 In order to obtain more compact and easier-to-use systems, the potential usage of smart materials (not  
63 requiring external pumps/motors) is of growing interest. In particular, within the family of  
64 electromechanically active polymers (Carpi 2016), dielectric elastomer actuators (DEAs) at present  
65 can in general offer large strains (10-100%) and relatively high stresses (up to 1 MPa) in response  
66 electrical stimuli, with simple structure, compact size, light weight and low power consumption  
67 (Carpi et al. 2008; Pelrine et al. 2000). Due to these attractive properties, their potential also for the  
68 mechano-stimulation of cells has recently been explored (Imboden et al. 2019; Poulin et al. 2018;  
69 Poulin et al. 2016; Cei et al. 2016; Akbari and Shea 2012,a; Akbari and Shea 2012,b). However, so  
70 far, they have been used for cell stretching of planar (uni- or bi-directional, or radial) and uniform  
71 kind. As a difference, tissues in vivo mostly undergo stretch fields that are non-planar, anisotropic  
72 and inhomogeneous (Balestrini et al. 2010). So, the greatest potential of these smart materials to  
73 mimic physiologically-relevant conditions remains at present mostly unexplored.

74 Here, we target a mechanical stimulation of cellular cultures on surfaces having a dynamically  
75 controllable curvature. As an alternative to conventional hydraulic/fluidic systems that can achieve an  
76 analogous effect, we present a DEA-based modular device made of elastomeric membranes that are  
77 deformable electrically (i.e. their curvature can be dynamically tuned by purely electrical means),  
78 without any fluidic system. This new approach is shown to lead to compact, self-contained and noise-  
79 free bioreactors that do not require any additional external mechanical equipment, as detailed below.

## 80 **2 Methods**

81 The structure of the proposed bioreactor and its principle of operation are presented in Figures 1a,b.  
82 An elastomeric cell culture membrane is arranged on top of a fluid-filled chamber that contains also a  
83 soft actuator. With respect to conventional hydraulic/fluidic systems, the fluid here has a different  
84 function, as explained below. The cell culture membrane seals the chamber and is in contact with the  
85 fluid. When the actuator is off (no applied voltage), the membrane surface can either be flat or, if  
86 needed, have an initial pre-curvature (obtained by increasing the fluid volume). In response to an  
87 applied voltage, the actuator is able to vary the cell culture membrane's curvature, according to a  
88 variable displacement of the fluid confined underneath, as detailed below.

89



90

91 **Figure 1.** Proposed bioreactor with electrically deformable curved membrane: (a) exploded view of  
 92 the structure; (b) picture of an assembled prototype; (c),(d) schematic representation of the principle  
 93 of operation; (e) examples of displacement signals (culture membrane and actuator) in response to a  
 94 cyclic voltage.

95

96 The soft actuator consists of a special type of DEA, known as hydrostatically coupled dielectric  
 97 elastomer actuator (HC-DEA) (Carpi et al. 2010). It is obtained by combining two dielectric  
 98 elastomer circular films together and confining a coupling fluid between them, so as to obtain a  
 99 bubble-like shape. One membrane (the one at the top in Figure 1c) is made active by sandwiching it  
 100 between two compliant electrodes connected to a voltage source, while the other membrane (the one  
 101 at the bottom in Figure 1c) is passive. When a voltage is applied to the active membrane, the bubble-  
 102 like structure of the actuator deforms upwards (Figure 1d). This is due to an electrically induced  
 103 reduction of the active membrane's thickness and an increase in its area, while the passive membrane  
 104 buckles in the same direction as a result of the fluid-mediated coupling (Carpi et al.2010).

105 This electrically induced deformation of the actuator is then used to displace the second coupling  
 106 fluid confined above it (Figure 1d), so that the cell culture membrane can assume a controllable

107 curvature, depending on the magnitude of the applied voltage. It is worth noting that voltages of  
108 opposite polarity and same amplitude cause the same curvature, as the actuation pressure generated  
109 by the HC-DEA is dependent on the square of the applied voltage (Carpi et al. 2010), as for any other  
110 DEA (Carpi et al. 2008). It is also useful to remark that the actuator's structure could easily be  
111 modified by making both of its membranes active (i.e. providing both of them with electrodes) and  
112 independently controllable, so as to make it able to buckle in both directions: this would enable bi-  
113 directional displacements of the cell culture membrane, in order to obtain both tuneable convexities  
114 and tuneable concavities.

115 According to this principle of operation, a voltage (either static or dynamic) applied to the soft  
116 actuator can be used to generate a deformation of the cell culture membrane, stretching any adhered  
117 cells both circumferentially and radially. The supplementary video SV1 shows a prototype in action.

118 Prototypes of this device were manufactured as follows. For the actuator's active and passive  
119 membranes, a 1mm-thick acrylic-based elastomeric film (VHB™ 4910, 3M, USA) was biaxially pre-  
120 strained by 250% (i.e. 3.5 times pre-stretched), reaching an estimated thickness of about 82  $\mu\text{m}$ , and  
121 fixed to a plastic circular frame with an internal diameter of 50 mm. The active membrane's  
122 compliant electrodes were manufactured using a custom-made conductive ink, consisting of a  
123 dispersion of 9 wt% carbon black (Black Pearls 2000, Cabot, USA) in a silicone pre-polymer  
124 (MED4901, NuSil, USA) dissolved in isooctane (Sigma Aldrich) with a 1:1 volume ratio. The  
125 reagents were mixed using a planetary mixer (THINKY ARE-250, Intertronics, UK) and the  
126 resulting ink was sprayed with an airbrush onto the active membrane's surfaces, where the silicone  
127 matrix was cured, obtaining elastomeric electrodes.

128 The actuator was then assembled by pulling the passive membrane with a custom-build vacuum  
129 chamber, filling the resulting cavity with 15 ml of a fluid silicone pre-polymer (Transil 40,  
130 Mouldlife, UK) and finally closing the cavity with the active membrane. The adhesive properties of  
131 the VHB elastomeric film allowed for sufficient bonding. The two membranes and the fluid  
132 encapsulated between them formed a bubble-like structure, with the fluid acting as a hydrostatic  
133 coupling medium between the membranes.

134 The cell culture membrane was manufactured by film casting with a silicone elastomer (Silbione  
135 LSR 4305, BlueStar Silicones, Norway). It had a thickness of about 75  $\mu\text{m}$  and a diameter of 16.5  
136 mm. A fluid-mediated hydrostatic coupling was also established between the actuator and the cell  
137 culture membrane, so as to transfer motion from the former to the latter. For simplicity, the adopted  
138 fluid was the same silicone pre-polymer used inside the actuator. The cell culture chamber was fixed  
139 to the rest of the structure with screws, so as to simplify the interchangeability among different types  
140 of chambers, enabling system modularity.

141 The diameter of the cell culture membrane was smaller than that of the actuator. Therefore, the fluid  
142 mediated coupling between surfaces of different area resulted in a larger vertical displacement in the  
143 cell culture membrane with respect to that of the actuator. This effect (maximised by an  
144 incompressible fluid) is evident from the sample signals shown in Figure 1e. Hence, changing the  
145 size of the cell culture membrane could be used to change the maximum achievable curvature at the  
146 maximum voltage, for any given actuator size. Moreover, for any given size of the cell culture  
147 membrane, the achievable curvature can always be modulated via the applied voltage.

148 A preliminary characterisation of prototypes of this new device is presented below.

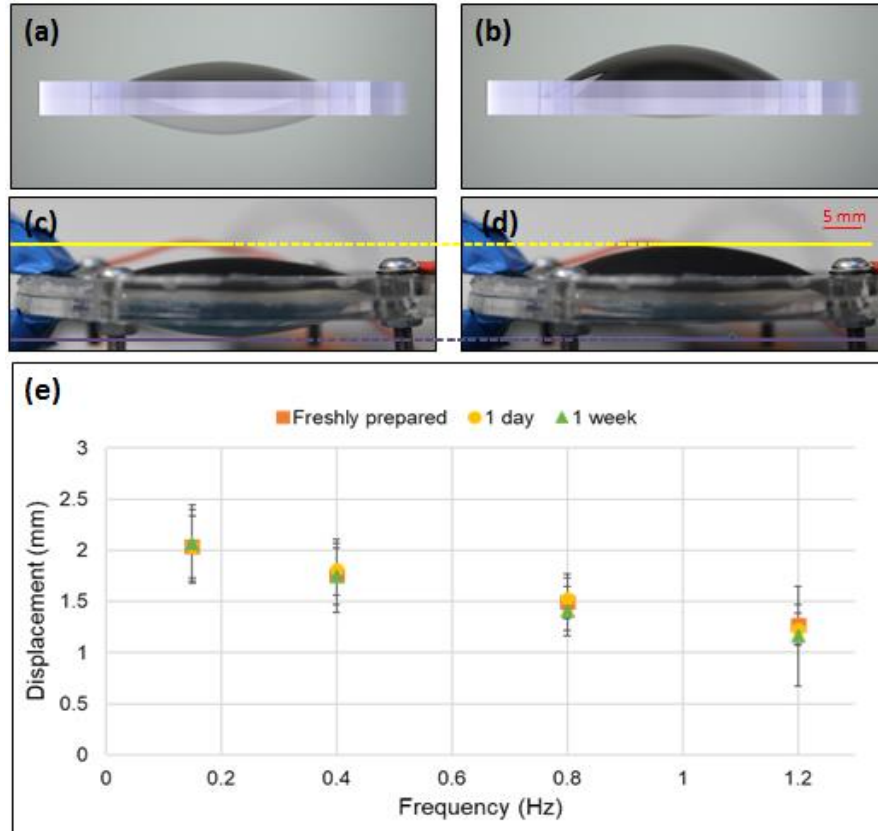
149

150 **3 Results and Discussion**

151 **3.1 Frequency response over time**

152 The HC-DEA dynamic performance was tested by measuring, with a laser-based displacement  
 153 transducer (optoNCDT 1800, Micro-Epsilon, Germany), the active membrane's maximum  
 154 displacement (Figure 2a-d) in response to unipolar sinusoidal voltages.

155



156

157 **Figure 2.** Operation of the HC-DEA and its frequency response. The drawings (a),(b) and pictures  
 158 (c),(d) of the device show it at electrical rest (a),(c) and with an applied voltage of 4.5 kV (b),(d).  
 159 Panel (e) presents the frequency response to 4.5 kV sinusoidal waves in terms of maximum  
 160 displacement of the central (highest) point of the active membrane, as measured at different times  
 161 after fabrication: 0, 1 and 7 days. Error bars represent the standard deviation among three samples.

162

163 As these tests were aimed at assessing the frequency response and how it changes over time, the  
 164 amplitude of the voltage signals was fixed (4.5 kV, according to the thickness of the active  
 165 membrane) and the frequency was varied within the 0.15-1.2 Hz range, corresponding to  
 166 characteristic frequencies of intestinal, lung and cardiac tissue motions (Saul 1990; Taylor and  
 167 Eckberg 1996; Han et al. 1998). The signals were obtained from a custom-made generator based on a  
 168 miniature high voltage multiplier (Q50, EMCO High Voltage Corporation, USA). For each tested

169 frequency, the voltage signal was applied for 3 minutes, followed by 1 minute of rest. The  
170 experiments were performed right after fabrication and then repeated after 1 and 7 days.

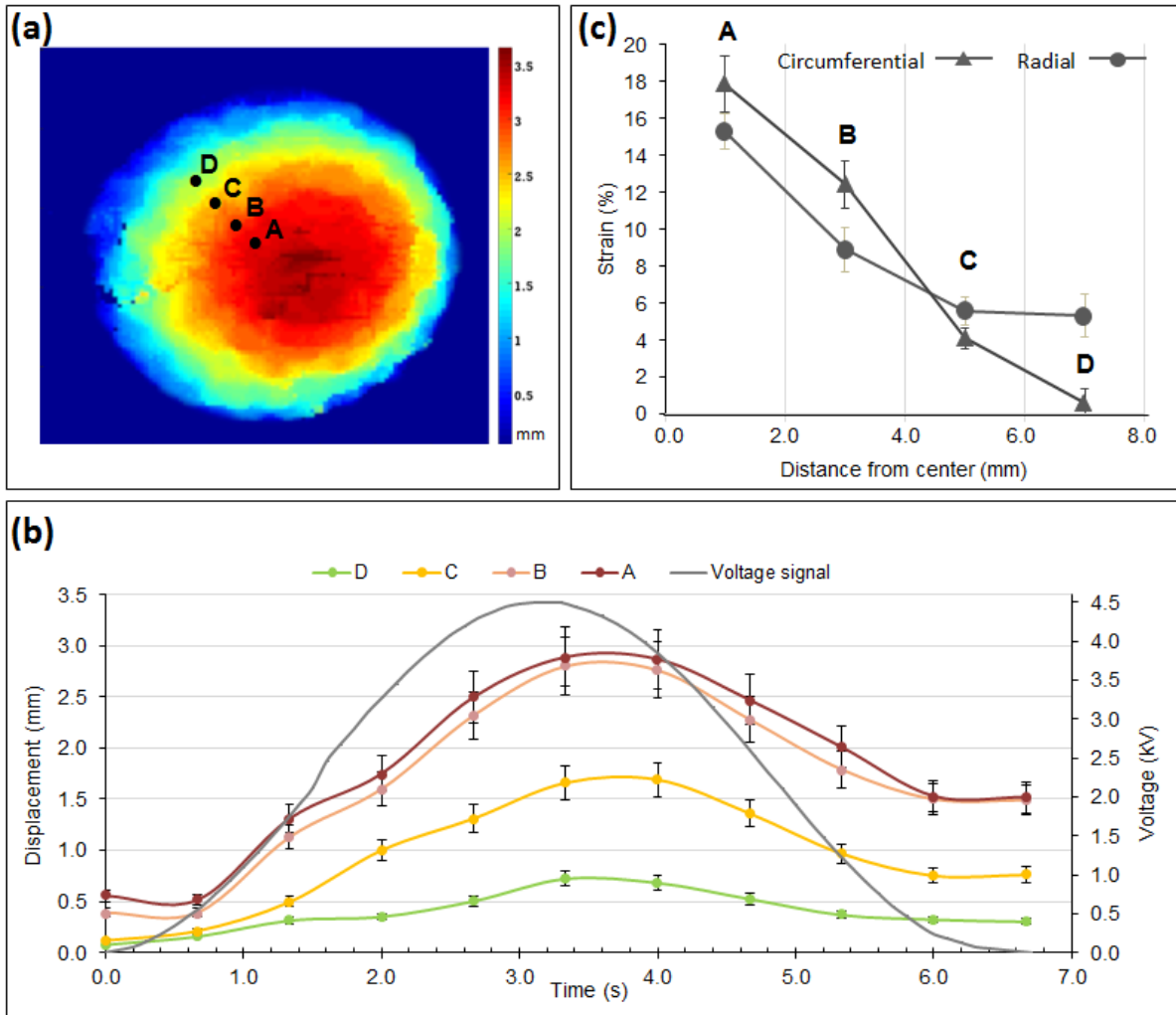
171 Figure 2e presents the results, showing that, as expected, there was a notable decrease of the  
172 achievable displacement as the frequency increased. This can be ascribed to the viscous components  
173 of the constitutive elastomeric membrane (Carpi et al. 2008). Nevertheless, for each frequency, the  
174 average displacement was found to be stable over time, at least over the 7 days investigated (Figure  
175 2e). This makes the technology potentially usable for continuous cell stretching over several days.

### 176 **3.2 Vertical displacements and radial and circumferential strains**

177 In order to investigate the deformation occurring in different regions of the cell culture membrane  
178 and thus assess the mechanical stimuli imposed to cells adhered over its surface, the following tests  
179 were performed.

180 The bioreactor was driven with a sinusoidal voltage of 4.5 kV at a frequency of 0.15 Hz and the bi-  
181 dimensional distribution of the vertical displacement (displacement field map) and mono-  
182 dimensional (radial) distribution of both the radial and circumferential strains were estimated.

183 Specifically, the displacement field map was defined as the spatial distribution of the maximum  
184 vertical displacement (during one actuation cycle) of the cell culture membrane across its surface. It  
185 was determined using a 3D optical mapping system based on two stereo cameras (LI-OV580-Stereo,  
186 Leopard Imaging, USA) that captured images at regular time steps, when the bioreactor was at rest  
187 and under electrical actuation. Figure 3a presents the resulting map, showing that the highest  
188 displacements occurred, as expected, in the central region, reaching about 3 mm. Figure 3b presents  
189 the time evolution of the vertical displacement during one actuation cycle, as measured from the four  
190 markers identified in Figure 3a. The comparison with the co-plotted voltage signals shows that the  
191 displacements had a delay of about 0.5 s. This can be ascribed to a combination of losses derived  
192 from the viscosity of the elastomer materials used for the actuator's and cell culture's membranes, as  
193 well as the inertia of the coupling fluid between them.



194

195 **Figure 3.** (a) Maximum displacement field map of the cell culture membrane for a sinusoidal voltage  
 196 at 4.5 kV and 0.15 Hz; (b) displacement signals captured from the four points identified in (a) during  
 197 one actuation cycle; (c) radial and circumferential strains estimated from the four markers shown in  
 198 (a). Note: the unexpectedly large radial strain at point D may be due to locally loose constraints close  
 199 to that edge, likely to have arisen from manufacturing defects. Error bars represent the standard  
 200 deviation among three samples.

201

202 In addition to the vertical displacement, the characterisation included the radial and circumferential  
 203 strains. Figure 3c presents their radial distribution, as estimated from the radial and circumferential  
 204 displacements of the four markers identified in Figure 3a. The estimation was attained through 3D  
 205 reconstructions by processing stereo images of the membrane at resting and deformed states.

206 As expected, both the strains were maximal in the central region of the membrane (about 18% for the  
 207 circumferential strain and 15% for the radial strain) and decreased along the radial direction towards  
 208 the edge. Nevertheless, it is worth stressing that this preliminary estimate of the strains was limited in  
 209 accuracy, as it used only four markers and so the values could not be averaged over a large data set.  
 210 This made the values particularly sensitive to defects inevitably introduced during the manual  
 211 fabrication of the device, especially at the edges, where the membrane was likely constrained with



212 anisotropic tension. This is evident, for instance, for the radial strain close to the edge (point D in  
 213 Figure 3c), whose unexpected high value was probably due to a local loss of tension, possibly  
 214 resulting in anomalous bumps.

215 **3.3 Mechanical stimulation of cell cultures**

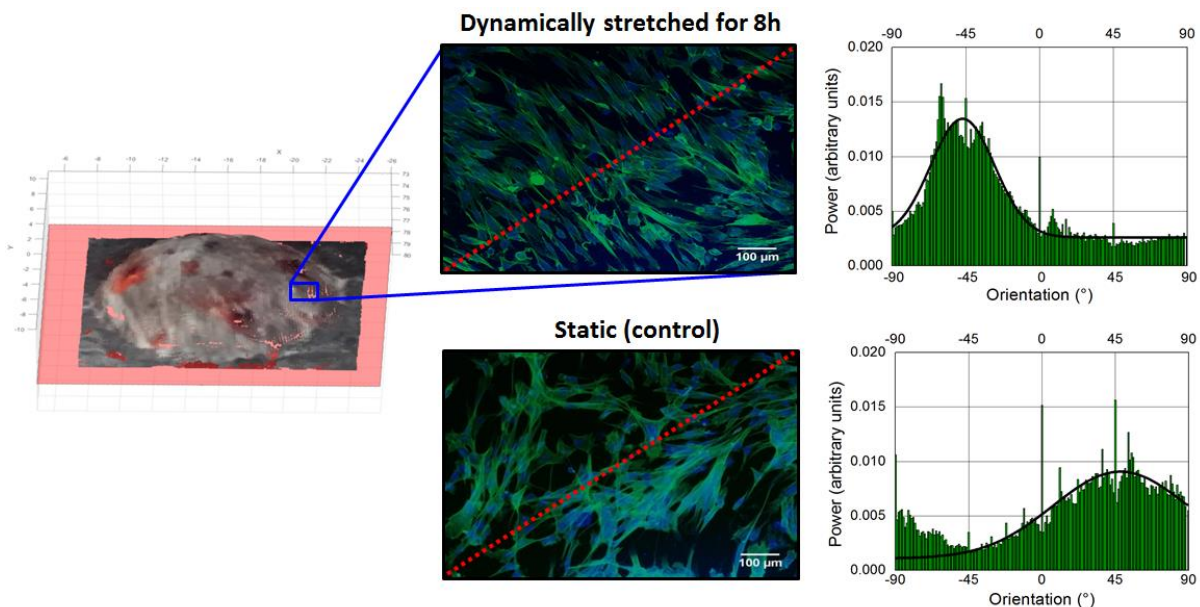
216 In order to verify the bioreactor’s ability to mechanically induce changes on cells adhering to its  
 217 surface, the following preliminary tests were conducted (all reagents were purchased from Sigma-  
 218 Aldrich).

219 Fibroblasts from the HFFF2 (Human Fetal Foreskin Fibroblasts 2) line were cultured in  
 220 supplemented 10% fetal bovine serum DMEM (Dulbecco’s modified eagle medium). Prior to cell  
 221 seeding, the cell culture membrane was coated with type I collagen from rat tail. Fibroblasts were  
 222 seeded at a density of 100,000 cells per bioreactor well and maintained in a cell culture incubator  
 223 (100% humidity, 37 °C, 5% CO<sub>2</sub>) for 24 h. Subsequently, the bioreactor was actuated inside the  
 224 incubator with a unipolar sinusoidal voltage of 4.5 kV at 0.15 Hz. The stimulation lasted 8 h, which  
 225 was considered sufficient to observe morphological changes in the cells, as it is known that  
 226 fibroblasts subject to stretch begin to orient within 3 h (Neidlinger-Wilke et al. 2002).

227 The control sample consisted of an identical bioreactor, containing cells with the same passage  
 228 number from the same cell batch, cultured in the same conditions, except for cyclic stretching (which  
 229 was not performed, as no voltage was applied).

230 At the end of the test, the cells were fixed with 4% paraformaldehyde and stained for actin  
 231 (phalloidin) and the nuclei (DAPI). The culture membrane was then imaged at different locations  
 232 using a fluorescence microscope (IX81, Olympus, Japan).

233 Figure 4 shows a typical outcome of this test, referring to a portion of the surface located between the  
 234 points C and D identified in Figure 3a. Following the stimulation, the cytoskeletal fibers (stained in  
 235 green) showed a distinct preferential orientation with respect to those of the control (non-stimulated)  
 236 sample.



237

238 **Figure 4.** Effect of cyclic stretching of fibroblasts for 8 h in the bioreactor: images of a cell culture  
239 membrane's patch (located between points C and D of Figure 3a), taken from both a dynamically  
240 stretched sample, just after stretching, (top) and the static sample of control (bottom). The red dashed  
241 lines indicate the radial direction. The graphs next to each image present the angular distribution of  
242 the cytoskeletal fibers.

243 In order to quantify this effect, the green-stained fiber alignment was measured via a Fourier  
244 component analysis performed by the Directionality plug-in of the Fiji – ImageJ open-source  
245 software. The angular orientation of the fibers was computed with respect to a  $0^\circ$  reference defined as  
246 the horizontal right-hand direction of the image, with angles increasing counter-clockwise. The  
247 results are plotted next to each image in Figure 4: the cells in the stretched sample had a pronounced  
248 preferential orientation, with a higher intensity (peaking at  $-47^\circ$ ) and a narrower dispersion ( $\pm 19^\circ$ )  
249 than those of the control sample (peaking at  $48^\circ$  with a dispersion of  $\pm 41^\circ$ ).

250 This preliminary investigation suggests that the HC-DEA-based bioreactor is able to induce a  
251 measurable effect on the orientation of the cytoskeleton and that this orientation tends to be  
252 perpendicular to the direction of the imposed radial stretch.

253 A more in-depth assessment of this effect will require systematic testing on a large number of  
254 samples, with a diversity of conditions of stimulation, which goes beyond the scope of this Brief  
255 Research Report. Nevertheless, it is worth noting that this outcome is in accordance with previously  
256 reported findings. Indeed, using other stimulation devices, fibroblasts have been shown to align  
257 perpendicularly to the direction of uniaxial cyclic stretch (Huang et al. 2013; Weidenhamer et al.  
258 2013). Kang et al. (Kang et al. 2011) suggested that when the actin filaments are cyclically stretched,  
259 a perpendicular alignment with respect to the direction of stretch emerges in response to nodal  
260 repositioning, to minimize net nodal forces from filament stress states. Similarly, other types of cells,  
261 such as lymphatic endothelial cells, have been reported to orient perpendicularly to a uniaxial 10%  
262 strain at 0.1 Hz applied for 24 h via a planar DEA-based device (Poulin et al. 2016).

263 Compared to previous studies, the new device proposed here offers a compact and versatile tool for  
264 applying strain fields that are not purely uniaxial, nor purely planar, without any additional  
265 mechanical equipment. This bioreactor could thus be used to investigate the response of cells  
266 stimulated by stretchable substrates undergoing out-of-plane deformations, thereby closer to several  
267 conditions *in vivo*.

### 268 3.4 Future developments

269 In addition to systematic testing, future developments should also optimise the actuation elastomer.  
270 In this study, the VHB acrylic by 3M was used to facilitate manufacturing, due to its adhesive  
271 properties, and take advantage of its high quasi-static electromechanical performance (Pelrine et al.  
272 2000). Nevertheless, its high viscosity not only limits the driving frequency to the order of 1 Hz  
273 (which however is not a problem for a bioreactor, considering that cells *in vivo* are never exposed to  
274 much higher frequencies), but also can cause a significant stress relaxation, especially with the high  
275 pre-strains required for optimal operation (Pelrine et al. 2000). Therefore, to avoid a possible  
276 reduction of performance over time, less viscous elastomers, like silicones, are a better choice (Maffli  
277 et al. 2015; Rosset et al. 2016), enabling devices that should last million cycles (Matysek et al. 2011).

278 Furthermore, improved manufacturing is necessary to reduce manual procedures, which in this work  
279 inevitably determined the variability of performance evidenced by the error bars in Figs. 2e and 3.

280 The main drawback of this technology is the need for high voltages (kV), although they have  
281 different implications, as discussed below, on the electrical driving units, the cultured cells, the  
282 operators and co-located electronics.

283 In terms of driving units, the generation of such voltages is not technically problematic, as the  
284 bioreactor does not require high powers and high frequencies. Indeed, the actuator is a capacitive  
285 load, which does not absorb high power, and the order of magnitude of frequencies needed for  
286 biomimetic cellular stretching is not greater than 1 Hz. For these reasons, in this work it was possible  
287 to use the high voltage multiplier by EMCO, which generates up to 5 kV at 0.5 W from an input  
288 signal up to 5 V, with a limited bandwidth (about 1 Hz) and a volume of about 2 cm<sup>3</sup>. Therefore, this  
289 kind of bioreactor can be controlled with battery-operated compact units.

290 In terms of interference with cell function, it is worth noting that the culture membrane is not  
291 exposed to the high electric field that builds up between the actuation electrodes. Indeed, the main  
292 field is confined within the actuation membrane, whilst the fringe field is not expected to impact the  
293 cell culture, due to the geometry of the device. In any case, it is useful to consider that previous  
294 studies on DEA-based cell stretchers, which have exposed cells to high fringe fields, have not  
295 obtained evidence of any effect on cellular (cardiomyocytes) viability (Imboden et al. 2019).

296 In terms of safety for the operators and for electronics which may be connected to the bioreactor (e.g.  
297 recording/stimulation electrodes and sensor probes), high voltages introduce the risk of electrostatic  
298 discharges (at a low power), which are unpleasant for humans and potentially destructive for  
299 electronics. This requires proper insulation of all the high voltage parts, including the voltage  
300 multiplier and the leads to the bioreactor. In this work, the high voltage unit was located outside the  
301 incubator and had thin cables arranged under the incubator's closed door. As a future simplification,  
302 the compact unit could be sealed within the bioreactor's case, obtaining a self-contained system,  
303 which could safely be used inside the incubator.

304 So, overall, there are no practical or safety concerns that should discourage the use of this technology  
305 just because of the high voltages. Nevertheless, they certainly are a drawback, not only because they  
306 bear the risk of electrostatic discharges (e.g. in case of breakdowns), but also because they make the  
307 electrical unit bulkier and more expensive than what it could be if the voltages were reduced by one  
308 order of magnitude. So, future developments should target a decrease of the voltages to a few  
309 hundred Volts. The critical threshold is around 250 V, which is related to low-size and low-cost  
310 drivers available for several piezoelectric transducers. To this end, efforts are needed to manufacture  
311 reliable DEA membranes with a thickness reduced to a few microns. Although this is challenging,  
312 the feasibility has already been proved (Poulin et al. 2015). However, as a lower thickness would  
313 reduce the membrane's stiffness, it will be necessary to stack multiple thin dielectric layers  
314 intertwined to compliant electrodes, so as to enable both low voltages and adequate stiffness.

#### 315 **4 Conclusions**

316 We described a novel bioreactor to cyclically stretch cells in vitro, via electrically deformable  
317 elastomeric membranes with a dynamically tuneable curvature. As compared to state-of-the-art  
318 devices, this bioreactor avoids the need for external pneumatic/fluidic drivers or electrical motors,  
319 which typically make the whole system bulky and difficult to operate. The electrical tuneability of  
320 the membranes is advantageous to obtain compact, self-contained, lightweight and versatile devices.

321 The bioreactor has a modular structure with an interchangeable cell culture unit analogous to that of  
322 multi-well plates, enabling the use of standard cell assays.

323 We demonstrated that cyclic stretching for 8 h could induce significant changes in the directionality  
324 of fibroblast cytoskeletal fibers, encouraging systematic investigations of this new technology.

325 Although previous studies have already introduced dielectric elastomer actuation for cell stretching,  
326 the new configuration described here can generate strain fields that are not purely uniaxial, nor purely  
327 planar, but are instead based on the modulation of the cell culture membrane's curvature. This feature  
328 opens up new opportunities to exploit this smart-material-based actuation technology to mimic  
329 complex 3D deformations occurring in vivo, such as those related to pulmonary inflation, cardiac and  
330 vascular pulsation and gastro-intestinal peristalsis.

### 331 **5 Conflict of Interest**

332 The authors declare that the research was conducted in the absence of any commercial or financial  
333 relationships that could be construed as a potential conflict of interest.

### 334 **6 Author Contributions**

335 F.C., J.C. and M.G. conceived the work. F.C., J.C.B. and A.A. supervised the work. J.C. and M.G.  
336 developed the bioreactor and performed the experiments. V.M. and V.F. measured the strains. F.C.  
337 and J.C. wrote the paper, with contributions from A.A. and J.C.B.

### 338 **7 Funding**

339 Financial support is gratefully acknowledged by J. Costa from the company IVTech S.r.l., Italy and  
340 by M. Ghilardi from the European MSCA-ITN-2014-Iarie Sklodowska-Curie Innovative Training  
341 Network Programme ("MICACT - MICroACTuators" project, grant agreement 641822).

### 342 **References**

343 Akbari, S. and Shea, H.R. (2012,a). Microfabrication and Characterization of an Array of Dielectric  
344 Elastomer Actuators Generating Uniaxial Strain to Stretch Individual Cells. *Journal of*  
345 *Micromechanics and Microengineering* 22 (4): 045020. [https://doi.org/10.1088/0960-](https://doi.org/10.1088/0960-1317/22/4/045020)  
346 [1317/22/4/045020](https://doi.org/10.1088/0960-1317/22/4/045020).

347 Akbari, S., and Shea, H.R. (2012,b). An Array of 100 $\mu\text{m}$ ×100 $\mu\text{m}$  Dielectric Elastomer Actuators  
348 with 80% Strain for Tissue Engineering Applications. *Sensors and Actuators A: Physical* 186  
349 (October): 236–41. <https://doi.org/10.1016/j.sna.2012.01.030>.

350 Balestrini, J. L., Skorinko, J.K., Hera, A., Gaudette, G.R., and Billiar, K.L. (2010). Applying  
351 Controlled Non-Uniform Deformation for in Vitro Studies of Cell Mechanobiology. *Biomechanics*  
352 *and Modeling in Mechanobiology* 9 (3): 329–44. <https://doi.org/10.1007/s10237-009-0179-9>.

353 Brown, T. D. (2000). Techniques for Mechanical Stimulation of Cells in Vitro: A Review. *Journal of*  
354 *Biomechanics* 33 (1): 3–14. [https://doi.org/10.1016/S0021-9290\(99\)00177-3](https://doi.org/10.1016/S0021-9290(99)00177-3).

355 Carpi, F., Frediani, G., De Rossi, D. (2010).Hydrostatically Coupled Dielectric Elastomer Actuators.  
356 *IEEE/ASME Transactions on Mechatronics* 15 (2): 308–15.  
357 <https://doi.org/10.1109/TMECH.2009.2021651>.

- 358 Carpi, F., De Rossi, D., Kornbluh, R., Pelrine, R., Sommer-Larsen, P. (2008). Dielectric Elastomers  
359 as Electromechanical Transducers: Fundamentals, Materials, Devices, Models and Applications of an  
360 Emerging Electroactive Polymer Technology. Fundamentals, Materials, Devices, Models and  
361 Applications of an Emerging Electroactive Polymer Technology. Oxford: Elsevier, UK.  
362 <https://doi.org/10.1016/B978-0-08-047488-5.X0001-9>.
- 363 Carpi, F. (2016). Electromechanically Active Polymers: A Concise Reference. Zurich: Springer  
364 International Publishing, Switzerland.
- 365 Cei, D., Costa, J., Gori, G., Frediani, G., Domenici, C., Carpi, F., Ahluwalia, A. (2016). A Bioreactor  
366 with an Electro-Responsive Elastomeric Membrane for Mimicking Intestinal Peristalsis.  
367 *Bioinspiration & Biomimetics* 12 (1): 16001. <https://doi.org/10.1088/1748-3190/12/1/016001>.
- 368 Clark, W. W., Smith, R., Janes, K., Winkler, J., Mulcahy, M. (2000). Development of a  
369 Piezoelectrically Actuated Cell Stretching Device. *Proc. SPIE, Smart Structures and Materials 2000:*  
370 *Industrial and Commercial Applications of Smart Structures Technologies*, 3991: 3991–98.  
371 <https://doi.org/10.1117/12.388171>.
- 372 Elsaadany, M., Harris, M., Yildirim-Ayan, E. (2017). Design and Validation of Equiaxial Mechanical  
373 Strain Platform, EQUicycler, for 3D Tissue Engineered Constructs. *BioMed Research International*  
374 2017: 3609703. <https://doi.org/10.1155/2017/3609703>.
- 375 Flexcell International. Online: <https://www.flexcellint.com>. Accessed on October 3, 2019.
- 376 Griffith, L. G. and Swartz, M.A. (2006). Capturing Complex 3D Tissue Physiology in Vitro. *Nature*  
377 *Reviews Molecular Cell Biology* 7(3): 211-24. <https://doi.org/10.1038/nrm1858>.
- 378 Han, O., Li, G.D., Sumpio, B.E., Basson, M.D. (1998). Strain Induces Caco-2 Intestinal Epithelial  
379 Proliferation and Differentiation via PKC and Tyrosine Kinase Signals. *The American Journal of*  
380 *Physiology* 275 (3): 534–41. <https://doi.org/10.1152/ajpgi.1998.275.3.G534>.
- 381 Huang, C., Miyazaki, K., Kaishi, S., Watanabe, A., Hyakusoku, H., Ogawa, R. (2013). Biological  
382 Effects of Cellular Stretch on Human Dermal Fibroblasts. *Journal of Plastic, Reconstructive &*  
383 *Aesthetic Surgery : JPRAS* 66 (12): e351-61. <https://doi.org/10.1016/j.bjps.2013.08.002>.
- 384 Kang, J., Steward, R. L., Kim, T., Schwartz, R. S., LeDuc, P. R., Puskar, K. M. (2011). Response of  
385 an Actin Filament Network Model under Cyclic Stretching through a Coarse Grained Monte Carlo  
386 Approach. *Journal of Theoretical Biology* 274 (1): 109–19.  
387 <https://doi.org/https://doi.org/10.1016/j.jtbi.2011.01.011>.
- 388 Kim, H. J., Huh, D., Hamilton, G., Ingber, D.E. (2012). Human Gut-on-a-Chip Inhabited by  
389 Microbial Flora That Experiences Intestinal Peristalsis-like Motions and Flow. *Lab on a Chip* 12  
390 (12): 2165–74. <https://doi.org/10.1039/c2lc40074j>.
- 391 Imboden, M., De Coulon, E., Poulin, A., Dellenbac, C., Rosset, S., Shea, H. & Rohr, S. (2019). High-  
392 speed mechano-active multielectrode array for investigating rapid stretch effects on cardiac tissue.  
393 *Nature Communications*, 10: 834. <https://doi.org/10.1038/s41467-019-08757-2>.
- 394 Leung, D.Y., Glagov, S., Mathews, M.B. (1977). A New in Vitro System for Studying Cell Response  
395 to Mechanical Stimulation. Different Effects of Cyclic Stretching and Agitation on Smooth Muscle

- 396 Cell Biosynthesis. *Experimental Cell Research* 109 (2): 285–98. [https://doi.org/10.1016/0014-4827\(77\)90008-8](https://doi.org/10.1016/0014-4827(77)90008-8).  
397
- 398 Maffli, L., Rosset, S., Ghilardi, M., Carpi, F. & Shea, H. (2015). Ultrafast All-Polymer Electrically  
399 Tunable Silicone Lenses. *Adv. Funct. Mater.* 25: 1656–1665.  
400 <https://doi.org/10.1002/adfm.201403942>.
- 401 Matysek, M., Lotz, P., Schlaak, H. F. (2011). Lifetime investigation of dielectric elastomer stack  
402 actuators. *IEEE Transactions on Dielectrics and Electrical Insulation*, 18(1): 89-96.  
403 <https://doi.org/10.1109/TDEI.2011.5704497>.
- 404 Meikle, M. C., Reynolds, J.J., Sellers, A., Dingle, J.T. (1979). Rabbit Cranial Sutures in Vitro: A  
405 New Experimental Model for Studying the Response of Fibrous Joints to Mechanical Stress.  
406 *Calcified Tissue International* 28 (2): 137–44. <https://doi.org/10.1007/bf02441232>.
- 407 Neidlinger-Wilke, C., Groot E., Claes, L., Brand, R. (2002). Fibroblast Orientation to Stretch Begins  
408 within Three Hours. *Journal of Orthopaedic Research* 20 (5): 953–56. [https://doi.org/10.1016/S0736-0266\(02\)00024-4](https://doi.org/10.1016/S0736-0266(02)00024-4).
- 410 Pavesi, A., Adriani, G., Rasponi, M., Zervantonakis, I.K., Fiore, G.B., Kamm, R.D. (2015).  
411 Controlled Electromechanical Cell Stimulation On-a-Chip. *Scientific Reports* 5 (July): 11800.  
412 <http://dx.doi.org/10.1038/srep11800>.
- 413 Pelrine, R., Kornbluh, R., Pei, Q. & Joseph, J. (2000) High-Speed Electrically Actuated Elastomers  
414 with Strain Greater Than 100%. *Science* 287, 836–839.  
415 <https://doi.org/10.1126/science.287.5454.836>.
- 416 Poulin, A., Demir, C.S., Rosset, S., Petrova, T. V., Shea, H. (2016). Dielectric Elastomer Actuator for  
417 Mechanical Loading of 2D Cell Cultures. *Lab on a Chip* 16 (19): 3788–94.  
418 <https://doi.org/10.1039/C6LC00903D>.
- 419 Poulin, A., Imboden, M., Sorba, F., Grazioli, S., Martin-Olmos, C., Rosset, S., Shea, H. (2018). An  
420 Ultra-Fast Mechanically Active Cell Culture Substrate. *Scientific Reports* 8 (1): 9895.  
421 <https://doi.org/10.1038/s41598-018-27915-y>.
- 422 Poulin, A., Rosset, S. & Shea, H. R. (2015) Printing low-voltage dielectric elastomer actuators. *Appl.*  
423 *Phys. Lett.* 107: 244104. <https://doi.org/10.1063/1.4937735>.
- 424 Rosset, S. & Shea, H. R. (2016). Small, fast, and tough: Shrinking down integrated elastomer  
425 transducers. *Appl. Phys. Rev.* 3: 031105. <https://doi.org/10.1063/1.4963164>.
- 426 Saul, J.P. (1990). Beat-To-Beat Variations of Heart Rate Reflect Modulation of Cardiac Autonomic  
427 Outflow. *Physiology* 5 (1): 32–37. <https://doi.org/10.1152/physiologyonline.1990.5.1.32>.
- 428 Strex Inc. Online: <https://strexcell.com>. Accessed on October 3, 2019.
- 429 Taylor, J. A. and Eckberg, D.L. (1996). Fundamental Relations Between Short-Term RR Interval and  
430 Arterial Pressure Oscillations in Humans. *Circulation* 93 (8): 1527–1532.  
431 <https://doi.org/10.1161/01.cir.93.8.1527>

432 Weidenhamer, N. K. and Tranquillo, R.T. (2013). Influence of Cyclic Mechanical Stretch and Tissue  
433 Constraints on Cellular and Collagen Alignment in Fibroblast-Derived Cell Sheets. *Tissue*  
434 *Engineering. Part C, Methods* 19 (5): 386–95. <https://doi.org/10.1089/ten.TEC.2012.0423>.